

## Changes in the crystal structure of tsaregorodtsevite [N(CH<sub>3</sub>)<sub>4</sub>][Si<sub>2</sub>(Si<sub>0.5</sub>Al<sub>0.5</sub>)O<sub>6</sub>]<sub>2</sub> on heating

BARBARA L. SHERRIFF,<sup>1</sup> ELENA V. SOKOLOVA,<sup>2</sup> JANICE CRAMER,<sup>1</sup> GERALD KUNATH-FANDREI,<sup>3</sup>  
CHRISTIAN JÄGER,<sup>3</sup> AND LEONID A. PAUTOV<sup>4</sup>

<sup>1</sup>Department of Geological Sciences, University of Manitoba, Canada R3T 2N2

<sup>2</sup>Department of Crystallography, Faculty of Geology, Moscow State University, Moscow 119899, Russia

<sup>3</sup>Institut für Optik und Quantenelektronik, Friedrich-Schiller Universität, Max-Wien Platz 1, D-07743 Jena, Germany

<sup>4</sup>Mineralogical Museum, Il'men Natural Reserve, Miass 456301, Russia

### ABSTRACT

Tsaregorodtsevite [N(CH<sub>3</sub>)<sub>4</sub>][Si<sub>2</sub>(Si<sub>0.5</sub>Al<sub>0.5</sub>)O<sub>6</sub>]<sub>2</sub> is a unique feldspathoid with a tetramethylammonium (TMA<sup>+</sup>) organic cation in an ordered, sodalite-like framework of orthorhombic symmetry (*I*222) with *a* = 8.984(3), *b* = 8.937(2), and *c* = 8.927(2) Å. Here, <sup>13</sup>C cross polarization MAS and <sup>1</sup>H MAS NMR spectra give direct evidence that the organic material in the cavities in tsaregorodtsevite is TMA<sup>+</sup>. The <sup>27</sup>Al and <sup>29</sup>Si MAS NMR spectra, and XRD data show that the framework is well ordered with Si in the T1 and T2 sites and both Si and Al in the T3 site. Upon heating, the colorless tsaregorodtsevite crystals change color becoming yellow, then brown, and finally black. In this study <sup>1</sup>H, <sup>13</sup>C, <sup>27</sup>Al, and <sup>29</sup>Si MAS NMR, powder XRD, and electron microprobe analyses are used to investigate the structural changes in tsaregorodtsevite on heating. The cell dimensions and T-O bond lengths decrease, and there are two phase changes. At 690 °C, the TMA<sup>+</sup> molecule breaks down to form aromatic rings and acidic groups, possibly including benzene and the pyridinium ion, with ammonia and other gases produced. The Al-Si framework changes slightly to give a less well-ordered tetragonal structure (*I*422), with *a* = 8.925(1), *c* = 8.908(1) Å, and a small amount of Al enters a separate phase. After heating at 970 °C, the organic material has further broken down with little C and H visible by NMR spectroscopy. The Al-Si framework forms at least two new phases: one with a cubic crystalline structure (*I*432) with *a* = 8.817(3) Å, and an amorphous aluminosilicate phase. There is a small residue of the initial structure even after heating for one hour at over 900 °C.

### INTRODUCTION

Pauling (1930) studied the crystal structure of sodalite (Na<sub>4</sub>Al<sub>3</sub>Si<sub>3</sub>O<sub>12</sub>Cl) and proposed that its structure may be regarded as a collapsed derivative of a fully expanded framework of perfectly regular tetrahedra. Some 60 years after his prediction, a natural mineral, tsaregorodtsevite [N(CH<sub>3</sub>)<sub>4</sub>][Si<sub>2</sub>(Si<sub>0.5</sub>Al<sub>0.5</sub>)O<sub>6</sub>]<sub>2</sub>, was discovered by Pautov et al. (1993), with this fully expanded framework that contains an organic tetramethylammonium cation (TMA<sup>+</sup>) in the sodalite cage. This unique feldspathoid was found in the Man'-Khambo mountain ridge of the Polar Urals in association with quartz, anatase, albite, phillipsite, and rutile in the muscovite-chlorite schists (Pautov et al. 1993).

The topological similarity between the fully expanded framework of perfectly regular tetrahedra predicted by Pauling and the framework of sodalite was described in detail by Hassan and Grundy (1983, 1984). Sodalite that hosts organic molecules (including TMA<sup>+</sup>) has been synthesized and the dynamics of the TMA<sup>+</sup> group have been studied by NMR spectroscopy (Derouane and Nagy 1987, den Ouden et al. 1991).

A single crystal X-ray structure refinement of tsaregorodtsevite (Sokolova et al. 1991) showed that the structure is orthorhombic, space group *I*222, with *a* = 8.984(3), *b* = 8.937(2), *c* = 8.927(2) Å, and *V* = 716.8(5) Å<sup>3</sup> (Table 1). The structure contains three crystallographically distinct tetrahedral sites, with Si in the T1 and T2 sites and Si and Al alternating in the T3 site, which form a framework with the composition [Si<sub>2</sub>(Si<sub>0.5</sub>Al<sub>0.5</sub>)O<sub>6</sub>]<sub>2</sub><sup>0.5-</sup> (Fig. 1). Cation order among the tetrahedral sites of the tsaregorodtsevite framework, with a Si:Al ratio of 5:1, results in the orthorhombic symmetry in contrast to the cubic symmetry of the sodalite structure with a Si:Al ratio of 1:1.

Tsaregorodtsevite is the first mineral found to contain the organic [N(CH<sub>3</sub>)<sub>4</sub>]<sup>+</sup> (TMA<sup>+</sup>) group. The TMA<sup>+</sup> groups are situated in the large zeolite-like cavities of the structure and serve as counter ions to the negatively charged framework. In the structure refinement by Sokolova et al. (1991), the axial complex 222 was found to coincide well with the TMA<sup>+</sup> tetrahedron symmetry. In sodalite-group minerals, this position is usually occupied by negatively charged ions such as Cl<sup>-</sup>, SO<sub>4</sub><sup>2-</sup>, and OH<sup>-</sup>.

**TABLE 1.** Structural parameters from XRD data for tsaregorodtsevite\*

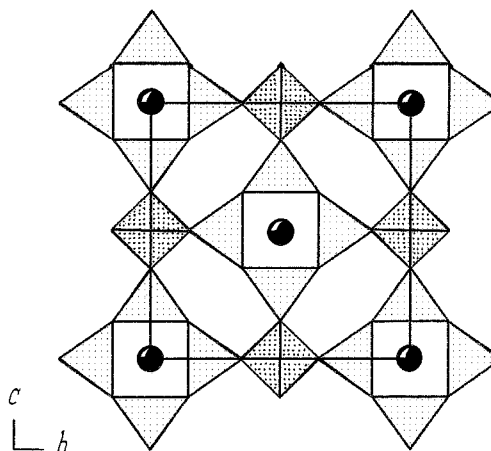
Experimental parameters	Unannealed	Annealed at 870 °C	Annealed at 940 °C
Space Group	I222	I422	I432
<i>a</i> (Å)	8.984(3)	8.908(1)	8.817(3)
<i>b</i> (Å)	8.937(2)		
<i>c</i> (Å)	8.927(2)	8.925(1)	
<i>V</i> (Å <sup>3</sup> )	716.8(5)	708.2(1)	685.5(4)
Ave. Si1-O (Å)	1.600	1.590	1.577
Ave. Si2-O (Å)	1.593	1.590	1.577
Ave. T3-O (Å)	1.630	1.626	1.577
Color	Colorless	Black	Black

\* From Sokolova et al. 1991.

Tsaregorodtsevite crystals are usually colorless, although they sometimes have a yellowish coloration. On heating, the crystals change color, becoming yellow, then brown, and finally black. Destruction of the TMA<sup>+</sup> groups upon heating to 870 °C was proposed as the cause of the change of color of the mineral (Sokolova et al. 1993). A differential thermal analysis study of the mineral reported one endothermic and several exothermic effects as well as a weight loss of about 9% at 870 °C (Pautov et al. 1993).

Structural refinements of the material produced after heating at 870 °C and 970 °C, using single-crystal X-ray diffraction (XRD) data, showed that there was a change of symmetry from orthorhombic, to tetragonal, and then to cubic (Sokolova et al. 1993). The tetragonal structure, which was stable at 870 °C, could be refined in space group *I422*, with unit-cell parameters *a* = 8.925(1), *c* = 8.908(1) Å, *V* = 708.2(1) Å<sup>3</sup> (Table 1). The cubic phase, which was produced when tsaregorodtsevite was heated above 900 °C, was refined in the space group *I432*, with unit-cell parameters *a* = 8.817(3) Å, *V* = 685.5(4) Å<sup>3</sup> (Table 1). The change in symmetry is accompanied by a decrease in unit-cell parameters resulting in a total decrease in the cell volume of 30 Å<sup>3</sup>, which is approximately 4% of the original volume (Table 1). Sokolova et al. (1991) also found a substantial change in the tetrahedral dimensions with these changes in symmetry, with the <T-O> distances decreasing progressively from 1.593, 1.600, and 1.630 Å, in the orthorhombic structure, to 1.590 and 1.626 Å in the tetragonal structure, and finally to 1.577 Å in the cubic structure. Sokolova et al. (1993) ascribed the change in symmetry, cell dimensions, and bond distances to the effect of increased Al-Si disorder in the framework.

However, the value of the tetrahedral cation-oxygen bonds (T-O) in the cubic phase is very short, even for an Si:Al ratio of 5:1, although, in milarite-group minerals, Si-O3 distances are 1.577 Å for sugillite and sogdianite and 1.583 Å for dusmatovite (Armbruster and Oberhansli 1988). They do, however, seem to be too short to allow for Al in the TO<sub>4</sub> tetrahedra unless there are many vacancies in the T and O sites. Unusually high values of displacement parameters for Si and O atoms, found by

**FIGURE 1.** The structure of tsaregorodtsevite viewed along the *a* axis. Light stipple = T1,T2; dark stipple = T3; spheres = N(CH<sub>3</sub>)<sub>4</sub><sup>+</sup>.

Sokolova et al. (1993), indicate possible deficiencies or disorder in both the tetrahedral and the O sites.

This study was undertaken to investigate some of the outstanding questions concerning the transformations of the tsaregorodtsevite structural framework upon heating and also to provide direct evidence for the speciation of the organic group within the zeolitic cavity both before and after heating. Both unheated and heated tsaregorodtsevite crystals were analyzed using the electron microprobe, which allowed the heterogeneity of the sample to be examined, on a scale of micrometers as well as providing a chemical analysis. Powder XRD patterns were examined for information about the long range structure and atomic ordering. Both <sup>29</sup>Si and <sup>27</sup>Al magic-angle-spinning nuclear magnetic resonance (MAS NMR) spectroscopy were used to study cation ordering of the framework. These are now well-established techniques for studying short range Al-Si ordering in aluminosilicate minerals (Phillips and Kirkpatrick 1994, Kohn et al. 1995, Sokolova et al. 1996). However, <sup>27</sup>Al MAS NMR spectra are usually less informative than <sup>29</sup>Si spectra because the peaks are often broadened and shifted by second-order quadrupolar effects. In this study, the spinning sidebands of the <sup>27</sup>Al satellite transitions are recorded and simulated to provide accurate chemical shifts and quadrupolar parameters. Although this is not the first report of the satellite transition technique (SATRAS), it is not widely used in mineralogical studies, and therefore the interpretation of the data is described in detail in this paper by comparing the spectra of tsaregorodtsevite with that of a well-ordered structure, AlPO<sub>4</sub>. In addition <sup>13</sup>C cross polarization (CP) MAS and <sup>1</sup>H MAS NMR spectroscopy were used to identify the organic structures in tsaregorodtsevite, both before and after heating.

## EXPERIMENTAL METHODS

### Materials

The colorless crystals of tsaregorodtsevite, from the Man'-Khambo mountain ridge in the Polar Urals, have a

cubic euhedral form. About one-half of the crystals used were transparent and one-half semi-transparent.

### Conditions for heating

The samples used for the NMR and powder XRD studies were heated for 40–60 min at 690 °C and at 970 °C at atmospheric pressure. They were then crushed manually to a fine powder in a pestle and mortar. The crystals used for electron microprobe analyses were heated at 640, 690, 760, 840, and 940 °C for about 1 h at atmospheric pressure.

### Electron microprobe analyses

Single crystals of tsaregorodtsevite, unheated and heated at 640, 690, 760, 840, and 940 °C, were mounted in epoxy resin, polished, and then analyzed using a CAMECA SX-50 electron microprobe operating at 15 kV and 20 nA with a beam diameter of approximately 1  $\mu\text{m}$  and count times of 20 s. The data reduction used the "PAP" procedure (Pouchou and Pichoir 1985) with diopside ( $\text{SiK}\alpha$ ), and kyanite ( $\text{AlK}\alpha$ ) as standards. Ten points were analyzed across the mineral surface, and average composition and standard deviations calculated for each grain.

### Nuclear magnetic resonance spectroscopy

The  $^{29}\text{Si}$  MAS and  $^{13}\text{C}$  CP MAS NMR spectra were obtained using a Doty high speed MAS probe with a Bruker AMX-500 multinuclear Fourier transform spectrometer console with two magnets operating at 8.4 and 11.7 T. Powdered samples of the mineral were spun at speeds of 6–8 kHz at an angle of 54.7° to the magnetic field. The  $^{29}\text{Si}$  MAS NMR spectra were recorded at a frequency of 99.3 MHz using the 11.7 T magnet with a spectral width of 50 kHz, 30° pulses, and delay of 5 s between pulses. Between 1000 and 10 000 scans were recorded for each spectrum. The  $^{13}\text{C}$  CP MAS spectra were recorded at a frequency of 90.5 MHz, using the 8.4 T magnet and spinning the sample at 6 kHz. The delay time between pulses was 5 s and the CP contact time was 9.5 ms. The spectra were  $^1\text{H}$  decoupled for 35.7 ms during the acquisition of between 400 to 10 000 free induction decays. Peak positions were measured with reference to tetramethylsilane (TMS) for  $^{29}\text{Si}$  and  $^{13}\text{C}$ . The relative intensities of the  $^{29}\text{Si}$  spectral peaks were found by integration.

The  $^1\text{H}$  MAS NMR spectra were obtained on a Bruker AMX 400 at a frequency of 400.1 MHz with a delay between pulses of 1 s. The numbers of scans recorded were 1000 for the unheated material and 2000–4000 for the heated samples.

The  $^{27}\text{Al}$  MAS NMR spectra were recorded using an AMX 400 spectrometer at a frequency of 104.26 MHz. Rotation rates of 14 kHz were applied using a Bruker 4 mm MAS probe. About 10000 to 20000 scans were accumulated with 0.1 s recycle delay. The spectra were referenced against the  $^{161}\text{Al}$  resonance of  $\text{Y}_3\text{Al}_5\text{O}_{12}$  (YAG) at

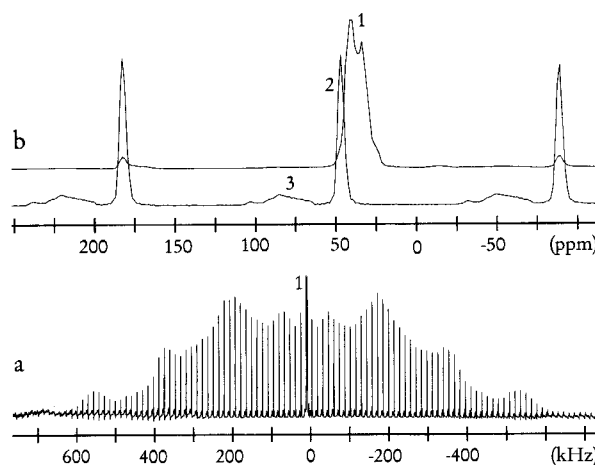


FIGURE 2. The  $^{27}\text{Al}$  MAS NMR spectrum. (a) Spinning sideband envelope of an  $\text{AlPO}_4$  (berlinite type) single crystal (1) denotes the position of the CT ( $C_q = 4.06$  MHz,  $\eta = 0.33$ ,  $\delta_{\text{iso}} = 40.6$  ppm). (b) Expansion of CT area (upper spectrum) and a part of the ST spinning sideband envelope over the same frequency range, scaled in intensity by a factor of 12.5; (1), (2), and (3) denote the CT,  $\frac{1}{2}$  ST, and  $\frac{5}{2}$  ST positions, respectively.

0.6 ppm (compared with  $^{161}\text{Al}$  in an aqueous solution of  $\text{AlCl}_3$ ).

Usually, in  $^{27}\text{Al}$  MAS NMR the lineshape of the so-called central transition (CT) ( $m = +\frac{1}{2} \leftrightarrow -\frac{1}{2}$ ) is acquired and then analyzed. Besides this, there are other transitions, which are referred to as satellite transitions (ST);  $m = \pm\frac{3}{2} \leftrightarrow \pm\frac{1}{2}$  (inner ST) and  $m = \pm\frac{5}{2} \leftrightarrow \pm\frac{3}{2}$  (outer ST). They can be observed, but their intensity is much lower in comparison with the CT spectrum because they are spread out over the range of the quadrupolar frequency (e.g., Engelhardt and Michel 1987). However, the MAS NMR lines of the inner ST offer an increased spectral resolution (Samoson 1985; Jäger 1994) because of reduced second-order quadrupolar broadening. These effects are illustrated by the  $^{27}\text{Al}$  MAS NMR lineshape of a powdered single crystal of  $\text{AlPO}_4$  (berlinite type; Fig. 2). This spectrum consists of a series of equally spaced ST spinning sidebands (Fig. 2a). The MAS line of the normally recorded CT (1) is situated in the middle of the ST spectrum (clipped in Fig. 2a). In Figure 2b it is compared with the third to fifth ST MAS sideband counted from the CT. These three ST MAS sideband groups are scaled to the CT MAS sidebands and belong to the inner (2) and outer (3) ST. Hence the strong lines in Figure 2a represent the inner ST. From their intensity distribution, the relevant quadrupole parameters can be obtained easily (Skibsted et al. 1991). For our  $\text{AlPO}_4$  sample the isotropic chemical shift  $\delta_{\text{iso}} = 40.6$  ppm, and the quadrupole coupling constant  $C_q = 4.06$  MHz with an asymmetry parameter  $\eta = 0.33$ . These values are in good agreement with the data published by Müller et al. 1984. For experimental details and applications of ST spectroscopy we refer to the literature (Kunath et al. 1992, Kunath-Fandrei et al. 1994, 1995a, 1995b; Jäger et al. 1993; Jäger 1994; Rehak

TABLE 2. Analytical data from EMP for tsaregorodtsevite

	Unheated	Heated at				
		640 °C	690 °C	740 °C	840 °C	940 °C
Al <sub>2</sub> O <sub>3</sub> wt%	11.19(0.10)	11.00(0.09)	11.16(0.08)	11.19(0.12)	11.65(0.12)	12.27(0.15)
SiO <sub>2</sub>	67.01(0.59)	67.93(0.66)	68.96(0.81)	69.27(0.63)	71.73(0.63)	74.43(0.84)
Total	78.20	78.93	80.13	80.47	83.37	86.70
Al (apfu)	1.03	1.00	1.00	1.00	1.00	1.02
Si (apfu)	5.23	5.25	5.25	5.25	5.25	5.24
Si:Al	5.1	5.2	5.2	5.2	5.2	5.1

et al., personal communication). The critical point to obtain a good spectrum is an accurate setting of the magic angle.

For acquiring the static <sup>27</sup>Al spectra, a  $\pi/2x-\pi/2y$  quadrupole echo pulse sequence was used with  $\pi/2$  pulse-lengths adjusted to 1.1  $\mu$ s and the delay  $\tau$  set to 25  $\mu$ s.

About 30 000 scans were recorded with a relaxation delay time of 100 ms.

### X-ray powder diffraction

X-ray powder patterns were collected, for the same powder samples that were used for the NMR spectra, on an ADP-2 diffractometer. CuK $\alpha$  radiation (Ni filter) was used with a step width ( $\Delta 2\theta$ ) of 0.02° and an exposure time of 5 s.

### RESULTS

The colorless crystals of tsaregorodtsevite turned yellow initially and then black on heating at 690 °C, and they remained black after heating for 1 h at 970 °C. There was a smell of amine when the mineral was crushed at room temperature for the NMR and powder XRD experiments.

### Electron microprobe analyses

The results of the electron microprobe analyses show that the Si:Al ratio is 5.1 rather than the value of 5.0 expected from the stoichiometric formula (Table 2). There is a systematic increase in total weight percentage of Al<sub>2</sub>O<sub>3</sub> and SiO<sub>2</sub> with temperature of heating, indicating that the mass loss because of the organic groups decreases, but there is no significant change in the atomic ratio of Si and Al. All the crystals of tsaregorodtsevite appeared to be homogeneous when observed with back-scattered electron imaging although the standard deviations of the measurements of weight percentage of oxides increase with temperature of heating.

### X-ray diffraction

The powder diffraction pattern of the unheated sample has narrow peaks indicating a very ordered structure (Fig. 3a). Upon heating to 690 °C, the peak positions remain the same, but the relative intensity changes and the peaks broaden by a factor of 1.5 indicating some disorder or site distortion (Fig. 3b). After heating at 970 °C, there are major differences in the powder X-ray pattern, with new peaks appearing (Fig. 3c). However, there is a small peak in the same position as the maximum intensity peak from the unheated sample. Both the original and new peaks are much weaker and broader than in the pattern of the unheated sample or the sample heated at 690 °C. The peaks are superimposed on a raised baseline (Fig. 3c).

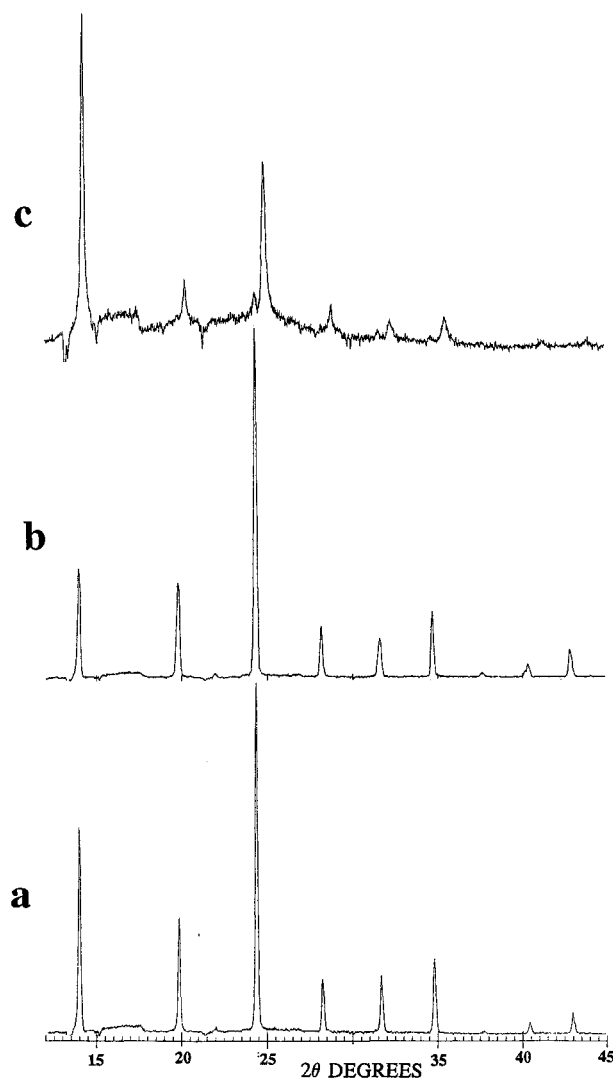


FIGURE 3. Powder XRD patterns of tsaregorodtsevite (a) unheated, (b) heated at 690 °C, and (c) heated at 970 °C.

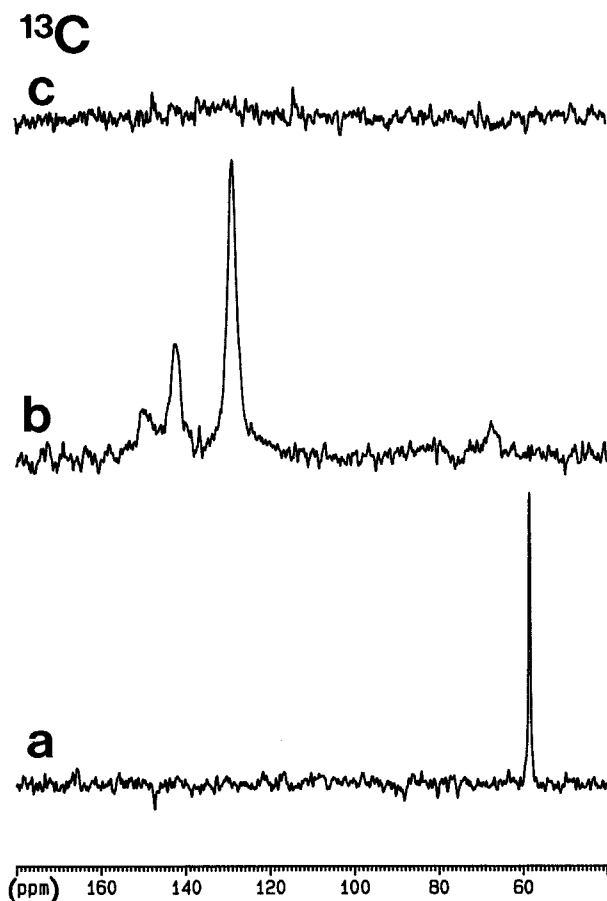


FIGURE 4. The  $^{13}\text{C}$  CP MAS NMR spectra of tsaregorodtsevite (a) unheated (383 scans), (b) heated at  $690^\circ\text{C}$  (1703 scans), and (c) heated at  $970^\circ\text{C}$  (10 971 scans).

#### $^{13}\text{C}$ CP MAS NMR spectroscopy

The  $^{13}\text{C}$  CP MAS spectrum of the unheated sample has a very narrow peak at 58.4 ppm with a full-width at half-maximum height (FWHM) of 50 Hz using a Gaussian line broadening (LB) of 20 Hz (Fig. 4a). After heating at  $690^\circ\text{C}$ , this peak completely vanished and was replaced by peaks at 128.7, 142.4, and 149.8 ppm with relative intensities of 5:2:1 and FWHMs of 400, 200, and 180 Hz (LB = 20 Hz) (Fig. 4b). Little is visible in the spectrum of the sample heated at  $970^\circ\text{C}$  except for a slight increase of the baseline in the aromatic region between 110 and 150 ppm (Fig. 4c).

#### $^1\text{H}$ MAS NMR spectroscopy

In the  $^1\text{H}$  MAS NMR spectrum of the unheated sample, a single narrow peak at 3.3 ppm is observed with a FWHM of 400 Hz (LB = 0 Hz) (Fig. 5a). A very small peak persists at this position (Fig. 5b and 5c) even after the sample is heated to  $960^\circ\text{C}$ . After heating at  $690^\circ\text{C}$ , there are three overlapping  $^1\text{H}$  resonances with apparently equal intensities at 9.2, 8.6, and 7.8 ppm with a smaller signal at 13 ppm, which is about 10% of the intensity of

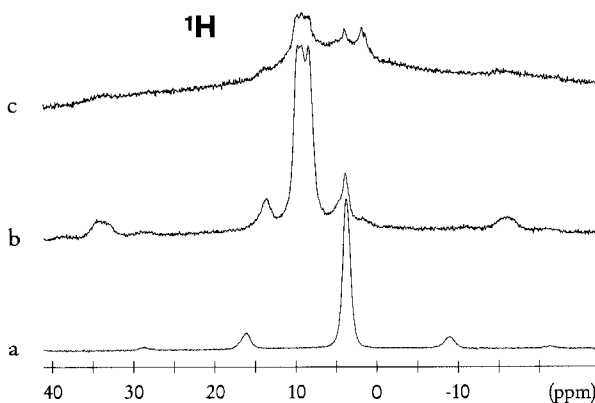


FIGURE 5. The  $^1\text{H}$  MAS NMR spectra of tsaregorodtsevite, (a) unheated, (b) heated at  $690^\circ\text{C}$ , and (c) heated at  $970^\circ\text{C}$ .

each of the main peaks (Fig. 5b). These peak positions remain constant with no significant change of relative intensity when the rotation frequencies were changed between 4 and 13 kHz, showing that they represent different chemical species and are not artifacts produced by the MAS technique.

The signal-to-noise ratio of the  $^1\text{H}$  spectrum is considerably reduced, after heating the sample at  $960^\circ\text{C}$  (Fig. 5c). The peaks have the same chemical shifts as described for the sample heated at  $690^\circ\text{C}$ . The weak additional peak at 1.2 ppm, caused by the Teflon rotor cap indicates the weakness of this spectrum, since it was not visible above the background noise in the other two  $^1\text{H}$  spectra.

#### $^{29}\text{Si}$ MAS NMR spectroscopy

There are two major peaks at  $-110.8$  ppm and  $-116.2$  ppm, with FWHMs of 250 and 130 Hz, respectively, in the  $^{29}\text{Si}$  MAS NMR spectrum of the unheated sample (Fig. 6a). There is also a small shoulder at  $-118$  ppm on the peak at  $-116$  ppm. The ratio of the peaks at  $-110$  and  $-116$  ppm was found to be 1:0.28. After the sample of tsaregorodtsevite was heated at  $690^\circ\text{C}$ , the two major peaks remain but they were broadened to 450 and 400 Hz, respectively. The shoulder at  $-118$  ppm appears to have increased in intensity (Fig. 6b), although the ratio of the two peaks remained at 1:0.28. In the spectrum of the sample heated at  $970^\circ\text{C}$ , the resolution of the individual peaks has been lost to give a broad asymmetrical resonance envelope with a FWHM of 1600 Hz centered at  $-110$  ppm (Fig. 6c). This spectrum was repeated with different values of relaxation delay in attempts to resolve two peaks. But these experiments were unsuccessful, and the non-gaussian distribution of a single resonance was always produced.

#### $^{27}\text{Al}$ SATRAS NMR spectroscopy

There is a single CT peak in the  $^{27}\text{Al}$  MAS spectrum with an isotropic chemical shift of 50.2 ppm (Fig. 7a, spectrum 1). Both the inner and outer ST MAS lines are detected for this sample (Fig. 7b, spectrum 1). The outer

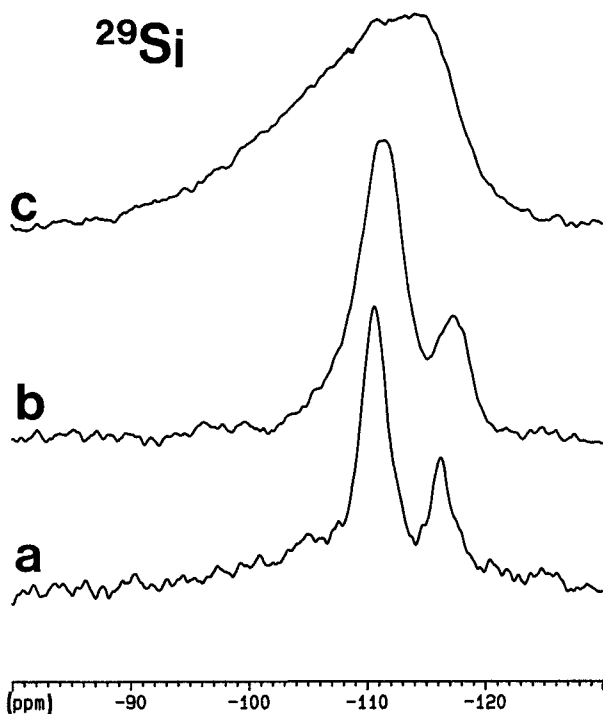


FIGURE 6. The  $^{29}\text{Si}$  MAS NMR spectra of tsaregorodtsevite, (a) unheated (6271 scans), (b) heated at  $690^\circ\text{C}$  (922 scans), and (c) heated at  $970^\circ\text{C}$  (10 177 scans).

MAS sidebands are on the left hand side of the strong inner ST MAS resonances.

After heating at  $690^\circ\text{C}$  the position of the  $^{27}\text{Al}$  resonance is unchanged although there is a small additional peak at about 13 ppm. The major CT resonance is broadened by a factor of two (Fig. 7a, spectrum 2), and simultaneously there is an extreme broadening of the ST MAS lines (Fig. 8c). A simulation of the envelope of the ST MAS lines yields a  $C_q$  value of 1.7 MHz and a distribution width of approximately 20%. The  $^{27}\text{Al}$  MAS lineshape of the sample heated to  $970^\circ\text{C}$  is unusual. Only about 5% of the Al remains in the original tetrahedral coordination (Fig. 7a, spectrum 3) whereas a strong and extremely broad second resonance occurs in the same position as the small additional peak at 13 ppm in the spectrum of the sample heated at  $690^\circ\text{C}$ .

## DISCUSSION

### NMR spectroscopy of the organic group

The peak at 58.4 ppm in the  $^{13}\text{C}$  CP MAS spectrum of the unheated sample of tsaregorodtsevite can be assigned to the methyl-carbon atoms in tetramethylammonium by comparison with the narrow peak obtained at 58.1 ppm by den Ouden et al. (1991) for a synthetic sample of  $\text{TMA}^+$ -containing sodalite. In the  $^1\text{H}$  MAS NMR spectrum of the unheated sample, the peak at 3.3 ppm can be allocated to the methyl protons of the  $\text{TMA}^+$  groups (den Ouden et al. 1991) (Fig. 5a). Den Ouden et al. (1991)

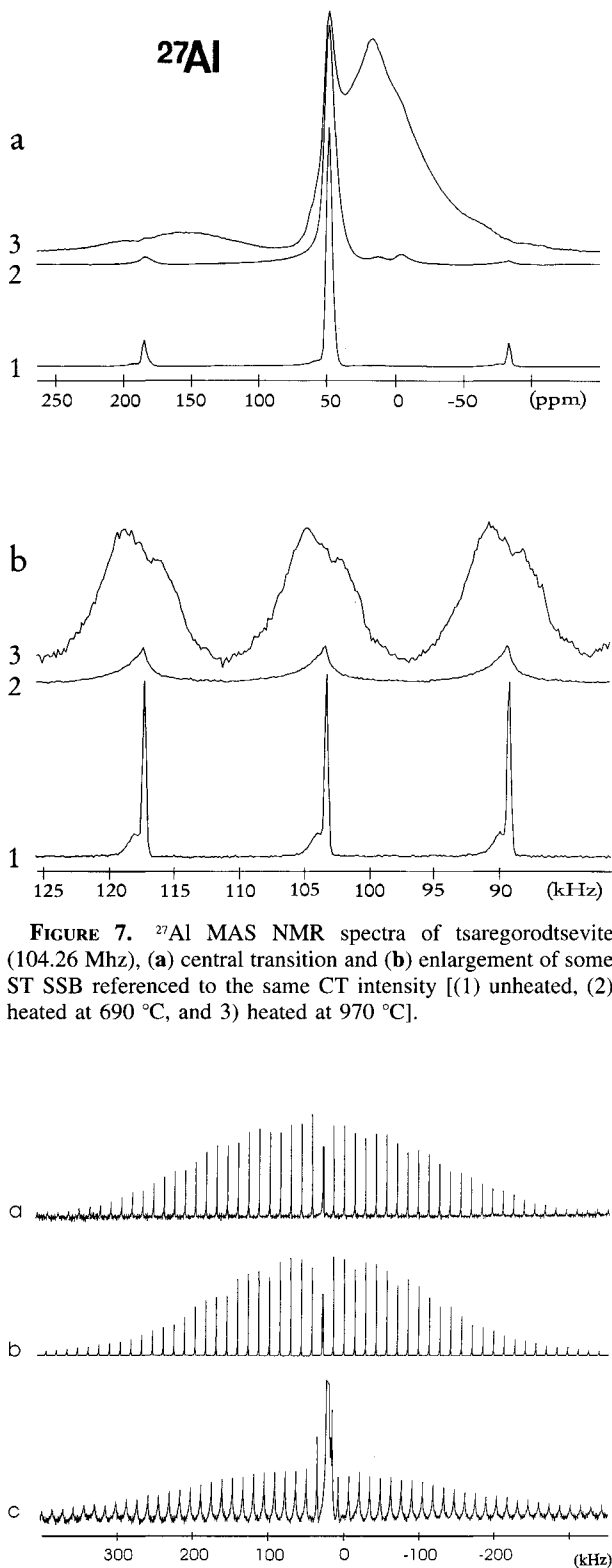


FIGURE 7.  $^{27}\text{Al}$  MAS NMR spectra of tsaregorodtsevite (104.26 Mhz), (a) central transition and (b) enlargement of some ST SSB referenced to the same CT intensity [(1) unheated, (2) heated at  $690^\circ\text{C}$ , and 3) heated at  $970^\circ\text{C}$ ].

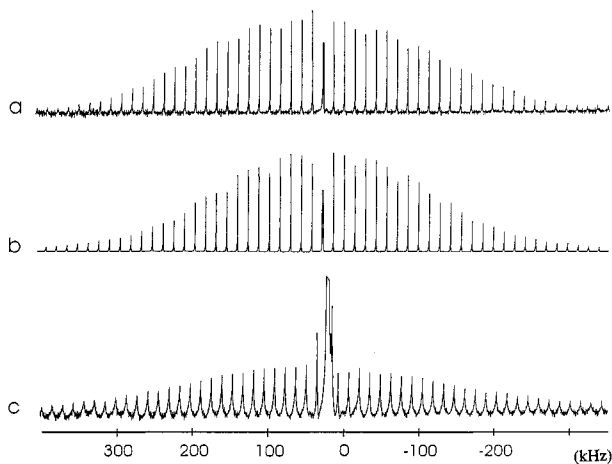


FIGURE 8. (a) The experimental  $^{27}\text{Al}$  ST sideband envelope of the unheated sample of tsaregorodtsevite; (b) a simulation with  $C_q = 1.68$  MHz, distribution (FWHM) = 8%; (c) experimental sideband envelope of the sample heated at  $690^\circ\text{C}$ .

calculated that the TMA<sup>+</sup> groups in a sodalite framework would rotate around the N-C bonds sufficiently rapidly on the microsecond NMR time scale to give average chemical shifts and narrow peaks. These NMR spectra are the first direct evidence of the presence of the TMA<sup>+</sup> group in a natural mineral and confirm the interpretation of the XRD data by Sokolova et al. (1991) about the identity of the organic ion present in tsaregorodtsevite.

After the sample was heated at 690 °C, new peaks appeared in both the <sup>13</sup>C CP MAS and <sup>1</sup>H MAS spectra and only a slight trace of the original peak is present in the <sup>1</sup>H spectrum. The presence of this peak in the spectra of the heated samples indicates that some of the original structure remains intact. This residue is not visible in the <sup>13</sup>C CP MAS spectra because of the relative insensitivity of <sup>13</sup>C compared with <sup>1</sup>H.

The new peaks at 7.8 ppm in the <sup>1</sup>H spectrum and at 128 ppm in the <sup>13</sup>C spectrum are in the same position as those of benzene (C<sub>6</sub>H<sub>6</sub>) (den Ouden 1991). One possible interpretation of the other peaks in these spectra is that they are due to the pyridinium ion (C<sub>5</sub>H<sub>5</sub>NH)<sup>+</sup>, which is formed by the replacement of one CH in benzene by NH<sup>+</sup>. The pyridinium ion in solution gives three <sup>13</sup>C peaks with chemical shifts of 148.4, 129.0, and 142.5 ppm in a ratio of 1:2:2 (Pretsch et al. 1989). The two smaller peaks found in the <sup>13</sup>C spectrum at 149.9 and 142.4 ppm have the approximate ratio 1:2. The peak at 128.7 ppm could be a combination of the signal from benzene and from the 129 ppm peak of the pyridinium ion. The <sup>1</sup>H chemical shifts for the pyridinium ion are 9.2, 9.0, and 8.5 ppm for the ring protons in a ratio of 2:1:2, and 10–12 ppm for the acidic proton adjacent to N (Pretsch et al. 1989). A range of shifts is given for the acidic proton because the value is dependant on the type of solvent. Peaks at 9.2 and 8.6 ppm are present in the <sup>1</sup>H spectrum in a ratio of approximately 1:1, as expected. The peak at 9.0 ppm is not visible but it would be less intense and therefore could contribute toward the two other peaks. The small, broad, high field peak at 13 ppm could be due to the acidic proton adjacent to N. This would be expected to be broadened, and therefore apparently less intense, because of quadrupolar and J coupling to <sup>14</sup>N.

Sokolova et al. (1993) found that ammonia was given off when tsaregorodtsevite was heated above 660 °C, as well as another water-soluble gas. The break down of the TMA<sup>+</sup> group on heating does therefore appear to be accompanied by the loss of N and H. The mechanism, whereby [N(CH<sub>3</sub>)<sub>4</sub>]<sup>+</sup> is transformed into C<sub>6</sub>H<sub>6</sub> and (C<sub>5</sub>H<sub>5</sub>NH)<sup>+</sup>, would require the migration of C and H and the loss of N from the system. The open framework structure of tsaregorodtsevite could facilitate such migration. At 690 °C, Al is still present in the framework so the presence of a charged species such as the pyridinium ion would aid in the stabilization of the negatively charged framework.

After heating the sample at 970 °C, the <sup>13</sup>C peaks have vanished and the <sup>1</sup>H spectrum is very weak. The totals of measured oxides in the electron microprobe analyses have

increased systematically on heating but still represent only 87% of the total mass of the mineral even after heating for 1 h at 970 °C. Therefore, some organic material is apparently still present. However, if most of the protons were removed during the heating process, as indicated by the considerable reduction in signal-to-noise ratio of the <sup>1</sup>H spectrum, there would be few protons remaining to cross-polarize with the <sup>13</sup>C. Therefore most of the intensity of the <sup>13</sup>C spectrum is lost despite the presence of carbon in the sample. The small peaks remaining in the <sup>1</sup>H spectrum have the same chemical shifts as described for the sample heated at 690 °C and are interpreted as being remnants of benzene and the pyridinium ion. The relative insensitivity of the <sup>13</sup>C CP MAS relative to <sup>1</sup>H explains the lack of corresponding peaks in the <sup>13</sup>C spectrum.

In summary, the <sup>13</sup>C CP MAS and <sup>1</sup>H MAS spectra prove that the initial organic structure is tetramethylammonium. Some of the TMA<sup>+</sup> groups break down on heating at 690 °C to form aromatic and hetero-aromatic groups, most probably a mixture of benzene and the pyridinium ion. Further heating at 970 °C destroys most of the groups that are visible by MAS NMR, although small residues of the TMA<sup>+</sup>, benzene and pyridinium ion, are still present even at this high temperature.

#### NMR spectroscopy of the Si-Al framework

The narrow peaks in the powder XRD pattern of the unheated sample become broader on heating. This indicates the very ordered structure (Fig. 3a) becomes disordered on heating. The new peaks, appearing after heating at 970 °C, are due to the structure with a cubic lattice and T-O distances of 1.577 Å, previously refined from single crystal X-ray data (Sokolova et al. 1993). The small peak in the same position as the maximum intensity peak from the unheated sample demonstrates that a small proportion of the original tsaregorodtsevite framework is still present, even after heating at 960 °C (Fig. 3c). The raised baseline in this pattern indicates the presence of amorphous material. The disorder or site distortion for the heated samples could be due to Si-Al disorder in the tetrahedral framework or among the organic groups in the cavities.

The largest peak at -110.8 ppm in the <sup>29</sup>Si MAS NMR spectrum of the unheated sample is assigned to the Si1 and Si2 sites that have identical (3Si 1Al) environments. The peak at -116.2 ppm is assigned to the third tetrahedral site (T3), which contains 0.5 Si and 0.5 Al and has four Si atoms surrounding it. The ratio of the peaks at -110 and -116 ppm was found to be 1:0.28. If the structure were perfectly ordered and stoichiometric the ratio should be 1:0.25. However, the electron microprobe analyses show a ratio of Si to Al of 5.1, which is 2% above the stoichiometric value of 5.0. Extra Si in the T3 sites would not only increase the intensity of the peak because of Si3 (4Si) at -116 ppm, but each Si replacing an Al in T3 causes the four Si1, Si2 (3Si 1Al) environments to have four Si neighbors instead. This would re-

sult in an extra peak, possibly the shoulder at  $-118$  ppm, which would be included in the integration of the peak at  $-116$  ppm. This double effect of excess Si in the T3 site would account for the 10% extra intensity of the high field peak.

In the unheated sample, XRD data indicate that only Al is in the T3 sites surrounded by four Si atoms, i.e., in an Al(4Si) configuration. This is supported by the fact that the  $^{27}\text{Al}$  CT MAS NMR peak is quite narrow and does not show second-order quadrupolar effects indicating that the quadrupolar coupling is rather small and the site symmetrical. On the other hand the complete ST MAS spectrum (Fig. 8a) shows a continuous decrease of the MAS sideband intensities when compared with the ST envelope of  $\text{AlPO}_4$  (Fig. 2a). Such a signal is typical for static distributions of the electric field gradient and hence of the quadrupolar coupling. The numeric simulation gave a mean coupling constant  $C_q$  of 1.68 MHz and a distribution width of about 8% (Fig. 8b). Similar spectra with even larger distributions of the interaction parameters were found for other polycrystalline materials, in particular for mullite (Kunath-Fandrei et al. 1994), where the distribution is a consequence of the substitution of Si by Al causing distortions of the coordination polyhedra. This kind of static effect could be assumed for tsaregorodtsevite because of the slight excess of Si in the T3 site. Although the  $\text{TMA}^+$  groups are known to have dynamic properties in the microsecond range (den Ouden 1991), the  $^{27}\text{Al}$  spectrum is obviously not influenced by this motion since it is fast relative to the MAS rotation period. In other words a fast rotation of this symmetrical molecule would cause a time-averaged electric-field gradient, and the NMR spectrum measures this averaged value. Under these circumstances we obtain MAS sidebands of the CT and ST transitions.

The broadening of the  $^{29}\text{Si}$  MAS NMR peaks, after the sample of tsaregorodtsevite was heated at  $690^\circ\text{C}$  (Fig. 6b), is indicative of increased disorder in the structure, either within the Al-Si framework or among the organic compounds in the framework cavities. The slight shift of the peaks to high field may be due to the changes occurring in the charge on the organic groups, which would affect the shielding strength of their electronic field. Tetramethylammonium has a net positive charge of one and would therefore have a deshielding effect in comparison with a neutral benzene group.

In the  $^{27}\text{Al}$  spectrum of the sample heated at  $690^\circ\text{C}$ , the position of the resonance is unchanged with heating, although there is a small additional peak at 13 ppm. The major CT resonance is broadened by a factor of two (Fig. 7a, spectrum 2) indicating that the environment of Al in the T3 site is changed slightly and less symmetrical. Simultaneously, an extreme broadening of the ST MAS lines is observed (Fig. 8c), which results in a distinct decrease of the sideband amplitudes.

The disappearance of ST MAS sidebands has been found in several materials, such as zeolites, sol-gel prepared materials, and glasses containing alkali ions. Sev-

eral explanations have been suggested. In zeolites, extremely large quadrupolar coupling constants (perturbations of the symmetry) and the effects of longitudinal relaxation times were discussed (Dougner et al. 1994; Freude et al. 1994), whereas in glasses motional processes of alkali ions are favored (Dirken et al. 1995). We have found this motional effect in various aluminosilicate glasses with several different alkali cations. If Li or Na is present the MAS sidebands disappear but K-containing glasses show the normal narrowing of the ST MAS lines. The MAS sidebands of the satellite transitions may disappear if the correlation time of the motion of a molecule is of the order of the MAS rotor period, provided that this molecular motion affects the electric field gradient. As the satellite transitions are broadened by first-order quadrupole interactions, their powder pattern extends over a frequency range of the order of the quadrupole frequency. Hence the MAS sidebands of these transitions are most sensitive to motional effects if the correlation times are comparable with the MAS rotor period. In other words, such motions result in little change of the electric field gradient symmetries or orientations, preventing the complete averaging of first-order effects over a rotor period. Because the quadrupole frequencies are much larger than the MAS frequency these small fluctuations severely broaden the ST MAS sidebands but not the CT MAS sidebands, since the first-order effects do not affect the CT.

In the spectrum of the sample heated at  $690^\circ\text{C}$ , we can exclude large symmetry distortions because the CT MAS pattern is still narrow (Fig. 7a, spectrum 2). To consider dynamic effects, we must search for molecules that show motional behavior with correlation times of the order of the rotor frequency, since the aluminosilicate framework of tsaregorodtsevite, or the structure produced on heating, should be too constrained to cause these motions. The  $^{13}\text{C}$  and  $^1\text{H}$  NMR revealed the presence of benzene and possibly the pyridinium ion. Various types of motion for benzene have been detected by NMR including a fast process with correlation times of  $10^{-8}$  s determined by  $^2\text{H}$  NMR measurements in Na-Y and Na-X zeolites (Auerbach et al. 1996), which should result in time-averaged electric field gradient tensors with no expected broadening of ST MAS lines. However, a discrete hopping process of the benzene molecule in the supercages of a Ca-LSX zeolite, on a time scale of the order of milliseconds, was detected by a 2D  $^{13}\text{C}$ -exchange NMR technique (Wilhelm et al. 1995). We assume that this motion of the benzene molecules is responsible for the broadening effects in the  $^{27}\text{Al}$  ST MAS lines of the tsaregorodtsevite sample heated at  $690^\circ\text{C}$ . A simulation of the envelope of the ST MAS lines yields a  $C_q$  value of 1.7 MHz and a larger distribution width, approximately 20%, which is in agreement with the analysis of the CT. This effect can also be correlated with the increased width of the  $^{29}\text{Si}$  peaks after heating at  $690^\circ\text{C}$ .

The odd-shaped peak in the  $^{29}\text{Si}$  spectrum of the sample heated at  $970^\circ\text{C}$  (Fig. 6c) is sufficiently broad to be due

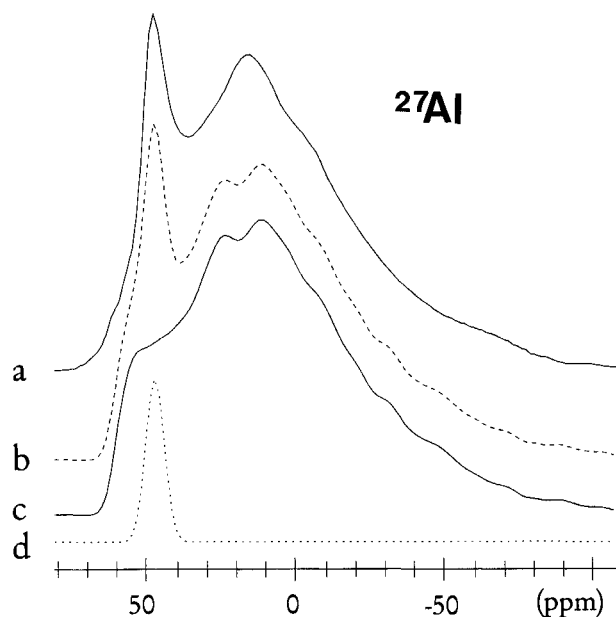


FIGURE 9. The  $^{27}\text{Al}$  CT fit of the spectrum of tsaregorodtsevite heated at 970 °C. (a) Experimental CT, (b) overall fit, (c) original site, and (d) assumed one site with  $C_q = 8.5$  MHz and isotropic chemical shift of 62 ppm.

to Si in an amorphous state (Sherriff and Fleet 1990). The asymmetry indicates that it may be a broad peak overlapping a narrow peak.

The  $^{27}\text{Al}$  CT MAS lineshape of the sample heated at 970 °C is again different. Only about 5% of the Al is left in the original tetrahedral coordination (Fig. 7a, spectrum 3), whereas a strong and extremely broad second resonance occurs in the same position as the small additional peak at 13 ppm in the spectrum of the sample heated at 690 °C. From the NMR point of view, the shape of the broad CT signal suggests a certain degree of order. Assuming a single signal, the CT can be simulated with an estimated quadrupole coupling of  $C_q \approx 8.5$  MHz (Fig. 9). Using this value of  $C_q$ , the chemical shift is calculated to be 62 ppm, indicating that this signal is also due to Al in tetrahedral coordination.

To get more information about these Al sites, an off-resonance MAS experiment at  $\pm 800$  kHz offset and a static quadrupole echo experiment were conducted. The lineshape of the ST MAS sidebands proves the presence of two sites with different quadrupole interactions (Fig. 10). The ST MAS sidebands for the Al site with the lower quadrupole coupling (right shoulder in Fig. 6b) vanish at about  $\pm 600$  kHz. This signal is identified with the original tsaregorodtsevite structure and makes up about 5% of the Al content as obtained from the CT MAS pattern. The ST MAS sidebands of the major resonance can be observed over more than 1.4 MHz on both sides of the CT. The ST envelope suggests a certain degree of short-range order in agreement with the analysis of the CT. A

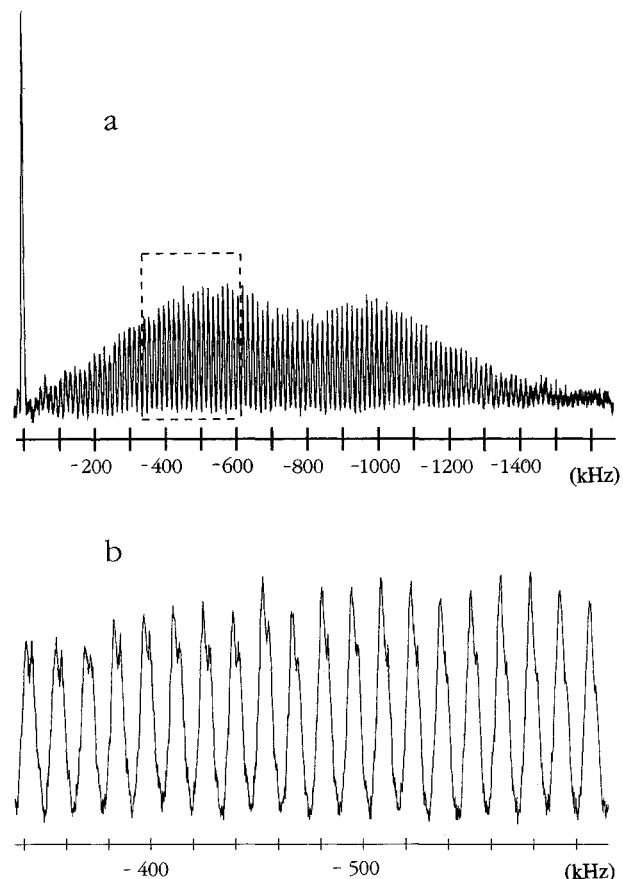


FIGURE 10. (a) The  $^{27}\text{Al}$  NMR experiment of the sample heated at 970 °C, taken at an offset of -800 KHz, showing the uncorrected ST envelope. (b) Expansion of the ST spinning sideband region.

static quadrupole echo experiment confirmed these findings.

#### Summary of structural changes on heating

Tsaregorodtsevite has a well-ordered aluminosilicate framework with Al in the T3 site, Si in the T1, T2, and T3 sites, and tetramethylammonium in the cavities in the structure. There is slight Si-Al disorder in the framework structure because of the excess Si in the T3 site above the stoichiometric value producing T1,T2 (4Si) environments. This is visible in the  $^{29}\text{Si}$  and  $^{27}\text{Al}$  NMR spectra but not in the XRD data or the backscattered EMP images. Therefore, this small amount of disorder is probably at a local atomic scale and there is no large scale manifestation such as the formation of domains or disruption of the long-range order visible by XRD.

When heated at 690 °C, the organic molecule breaks down and produces ammonia and other gaseous products. The residual C, H, and N form benzene and other heteroaromatic rings with acidic functional groups. The framework structure remains mostly unaltered but more disorder or site distortion is introduced causing an increased

broadening of the  $^{29}\text{Si}$  and  $^{27}\text{Al}$  CT peaks. Some breakdown of the framework at this temperature is shown by the extra peak in the  $^{27}\text{Al}$  spectrum and also by the change of space group from  $I222$  to  $I422$ . After breakdown, a small amount of Al is also in a secondary phase. The change from orthorhombic to tetragonal symmetry can be correlated with an increase in Si-Al disorder in the tetrahedral sites causing the T1 and T2 environments to be indistinguishable crystallographically as well as spectroscopically. Sokolova et al. (1991) found that, after heating crystals of tsaregorodtsevite at 870 °C, there was a reduction in the  $a$ ,  $b$ , and  $c$  unit-cell edges of 0.059, 0.29, and 0.019 Å, respectively. Because there was little change in the Si-Al composition observed in the electron microprobe analysis, this reduction can be related to the breakdown of the symmetrical  $\text{TMA}^+$  group.

After heating at 970 °C the organic compounds broke down further with the loss of most of the H, as shown by the very weak  $^1\text{H}$  MAS NMR spectrum. The lack of XRD lines from graphite or any other organic material indicates that the residual carbon and nitrogen were not formed into a structure with long-range crystallinity. This framework is not stabilized by the positively charged organic group and undergoes a phase change. However, even after one hour at this high temperature, there are still remnants of the original structure intact including the organic  $\text{TMA}^+$  group. The increased standard deviation for the values of weight percent  $\text{SiO}_2$  and  $\text{Al}_2\text{O}_3$  in the EMP analyses shows that there is more variation in the Si-Al analyses throughout the structure even though the ratios of Si to Al at any point remain constant. Therefore there are no domains or regions of high Al or Si concentration visible at the micrometer scale of the EMP.

Peaks of the new cubic structure are the major features of the XRD pattern but the raised baseline indicates the presence of an amorphous material. The broad  $^{29}\text{Si}$  MAS NMR signal could contain contributions from both crystalline and amorphous sites. The  $^{27}\text{Al}$  CT and ST MAS spectra indicate that the Al is in at least two tetrahedral environments, the original tsaregorodtsevite structure and a new amorphous one. The small peak at 13 ppm in the  $^{27}\text{Al}$  spectrum shows that this new environment had begun to form after heating at 690 °C.

We have now identified at least three environments for Si and Al in the sample heated at 970 °C: the original tsaregorodtsevite structure; a cubic structure with very short T-O bond distances, which may therefore contain only Si and O possibly with vacancies in both sites; and an amorphous phase containing Si and Al.

#### ACKNOWLEDGMENTS

We wish to acknowledge the assistance of Terry Wolowicz and Kirk Marat for assistance with the NMR data collection, Ron Chapman for the microprobe data, and Yurii Kabalov for the powder XRD data. Quadrupole NMR simulation software created mainly by Peter Losso (University of Jena) was used. The research was funded by a Natural Science and Engineering Research Council research grant and University Research Fellowship to B.L.S. and by a Russian Fund for Basic Research Grant number 95-05-15699 to E.V.S. G.K.F. and C.J. thank Deutsche Forschungsge-

meinschaft for financial support. We wish to thank three anonymous reviewers and J. Stebbins for helpful comments on an earlier version of this paper.

#### REFERENCES CITED

- Armbruster, T., and Oberhänsli, R. (1988) Crystal chemistry of double-ring silicates: Structures of sugilite and brannockite. *American Mineralogist*, 73, 595–600.
- Auerbach, S.M., Bull, L.M., Henson, N.J., Metiu, H.I., Cheetham, A.K. (1996) Behavior of benzene in Na-X and Na-Y zeolites: comparative study by  $^1\text{H}$  NMR and molecular mechanics. *Journal of Physical Chemistry*, 100, 5923–5930.
- Den Ouden, C.J.J., Datema, K.P., Vissar, F., Mackay, M., and Post, M.F.M. (1991) On the dynamics of organic-zeolite interactions: tetramethylammonium in sodalite. *Zeolites*, 11, 418–424.
- Derouane, E.G., and Nagy, J.B. (1987) Surface curvature effects of the NMR chemical shift for molecules trapped in microporous solids. *Chemical Physics Letters*, 137, 341–344.
- Dirken, P.J., Nachtgal, G.H., and Kentgens, A.P.M. (1995) Off-resonance nutation nuclear magnetic resonance study of framework aluminosilicate glasses with Li, Na, K, Rb, or Cs as charge-balancing cations. *Solid State Nuclear Magnetic Resonance*, 5, 189–200.
- Dougnier, F., Delmotte, L., and Guth, J.L. (1994) Observation of spinning sidebands in the  $^{27}\text{Al}$  MAS NMR spectra of FAU and EMT structure type zeolites. *Solid State Nuclear Magnetic Resonance*, 3, 331–338.
- Engelhardt, G., and Michel, D. (1987) High resolution solid state NMR of silicates and zeolites. John Wiley and Sons New York.
- Freude, D., Ernst, H., and Wolf, I. (1994) Solid state NMR studies of acid sites in zeolites. *Solid State Nuclear Magnetic Resonance*, 3, 271–286.
- Hassan, I., and Grundy, H.D. (1983) Structure of basic sodalite,  $\text{Na}_8\text{Al}_6\text{Si}_6\text{O}_{24}(\text{OH})_2 \cdot 2\text{H}_2\text{O}$ . *Acta Crystallography*, C39, 3–5.
- (1984) The crystal structures of sodalite-group minerals. *Acta Crystallography*, B40, 6–13.
- Jäger, C. (1994) Satellite transition spectroscopy of quadrupolar nuclei. *NMR Basic Principles and Progress*, 31, 133–170.
- Jäger, C., Kunath, G., Losso, P., and Scheler, G. (1993) Determinations of distributions of the quadrupole interaction in amorphous solids. *Solid State Nuclear Magnetic Resonance*, 2, 73–82.
- Kohn, S.C., Henderson, C.M.B., and Dupree, R. (1995) Si-Al order in leucite revisited: New information from an analcite-derived analogue. *American Mineralogist*, 80, 705–714.
- Kunath, G., Losso, P., Steuernagel, S., Schneider, H., and Jäger, C. (1992)  $^{27}\text{Al}$  satellite transition spectroscopy (SATRAS) of polycrystalline aluminium borate  $9\text{Al}_2\text{O}_3 \cdot 2\text{B}_2\text{O}_3$ . *Solid State Nuclear Magnetic Resonance*, 1, 261–266.
- Kunath-Fandrei, G., Rehak, P., Steuernagel, S., Schneider, H., and Jäger, C. (1994) Quantitative structural analysis of mullite by  $^{27}\text{Al}$  nuclear magnetic resonance satellite transition spectroscopy. *Solid State Nuclear Magnetic Resonance*, 3, 241–248.
- Kunath-Fandrei, G., Bastow, T.J., Hall, J.S., Jäger, C., and Smith, M.E. (1995a) Quantification of aluminum coordination in amorphous alumina by combined CT and ST MAS NMR. *Journal of Physical Chemistry*, 99, 15138–15141.
- Kunath-Fandrei, G., Bastow, T.J., Jäger, C., and Smith, M.E. (1995b) Quadrupole and Chemical Shift Interactions of  $^{27}\text{Al}$  in Aluminium Molybdate from Satellite Transition Magic Angle Spinning NMR. *Chemical Physics Letters*, 234, 431–436.
- Müller, D., Jahn, E., Ladwig, G., Haubenreisser, U. (1984) High resolution solid-state  $^{27}\text{Al}$  and  $^{31}\text{P}$  NMR; correlation between mean Al-O-P angle in  $\text{AlPO}_4$  polymorphs. *Chemical Physics Letters*, 109, 332–336.
- Pauling, L. (1930) The structure of sodalite and helvite. *Zeitschrift für Kristallographie*, 74, 213–225.
- Pautov, L.A., Karpenko, V.YU., Sokolova, E.V., and Ignatenko, K.I. (1993) Tsaregorodtsevite,  $\text{N}(\text{CH}_3)_4[\text{Si}_2(\text{Si}_6\text{Al}_6\text{O}_6)_2]$ , a new mineral. *Zapiski Vsesoyuznogo Mineralogicheskogo Obshchestva*, N1, 128–135.
- Phillips, B.L., and Kirkpatrick, R.J. (1994) Short-range Si-Al order in leucite and analcime: Determination of the configurational entropy from  $^{27}\text{Al}$  and variable temperature  $^{29}\text{Si}$  NMR spectroscopy of leucite, its Cs- and Rb-exchanged derivatives, and analcime. *American Mineralogist*, 79, 1025–1031.

- Pouchou, J.L., and Pichoir, F. (1985) "PAP" (phi-rho-Z) procedure for improved quantitative microanalysis. In J.T. Armstrong, Ed., *Microbeam analysis*, p. 104–106. San Francisco Press, California.
- Pretsch, E., Clerc, T., Seibl, J., and Simon, W. (1989) *Tables of spectral data for structure determination of organic compounds*,  $^{13}\text{C}$ -NMR,  $^1\text{H}$ -NMR, IR, MS, UV/VIS, 2nd edition Springer-Verlag, Berlin.
- Samoson, A. (1985) Satellite transition high-resolution NMR of quadrupolar nuclei in powders. *Chemical Physics Letters*, 119, 29–32.
- Sherriff, B.L., and Fleet, M.E. (1990) Local ordering in gallium- and germanium-substituted glasses investigated by MAS NMR. *Journal of Geophysical Research*, 95, B10, 15727–15732.
- Skibsted, J., Nielson, N.C., Bildsøe, H., and Jakobsen, H.J. (1991) Satellite transitions in MAS NMR spectra of quadrupolar nuclei. *Journal of Magnetic Resonance*, 95, 88–117.
- Sokolova, E.V., Rybakov, V.B., and Pautov, L.A. (1991) The crystal structure of a new natural tetramethylammonium aluminosilicate  $\text{N}(\text{CH}_3)_4[\text{Si}_2(\text{Si}_{10.5}\text{Al}_{0.5})\text{O}_6]_2$ . *Soviet Physics Doklady*, 36(4), 267–269.
- Sokolova, E.V., Rybakov, V.B., Pautov, L.A., and Pushcharovskii, D.Yu. (1993) Structural changes in tsaregorodtsevite. *Soviet Physics Doklady*, 38(9), 400–402.
- Sokolova, E. V., Kabalov, Y. K., Sherriff, B. L., Teertstra, D. K., Jenkins, D. M., Kunath-Fandrei, G., Goetz, S. and Jäger, C. (1996) Marialite: Rietveld structure refinement, and  $^{29}\text{Si}$  MAS and  $^{27}\text{Al}$  satellite transition NMR spectroscopy. *Canadian Mineralogist*, 34, 1039–1050.
- Wilhelm, M., Firouzi, A., Favre, D.E., Bull, L.M., Schaefer, D.J., and Chmelka, B.F. (1995) Dynamics of benzene adsorbed on Ca-LSX zeolite studied by solid state two dimensional exchange  $^{13}\text{C}$  NMR. *Journal of the American Chemical Society*, 117, 2923–2924.

MANUSCRIPT RECEIVED FEBRUARY 15, 1996

MANUSCRIPT ACCEPTED DECEMBER 24, 1996